C.P. No. 366
(18,373)
A.R.C Technical Report

C.P. No. 366
(18,373)
A R.C Technical Report

MINISTRY OF SUPPLY

AERONAUTICAL RESEARCH COUNCIL

CURRENT PAPERS

Turbulence Measurements in Supersonic Flow with the Hot-Wire Anemometer

By

B. Wise and D. L. Schultz,

Oxford University Engineering Laboratory

LONDON HER MAJESTY'S STATIONERY OFFICE

1957

FOUR SHILLINGS NET

C.P. No. 366

Turbulence Measurements in Supersonic Flow with the Hot-Wire Anemometer

- By -
B. Wise and D. L. Schultz,
Oxford University Engineering Laboratory.

O.U.E.L. Report No.83

Communicated by Professor A. Thom

December, 1955

SUMMARY

Previous measurements of turbulence under compressible flow conditions have shown that fluctuations in stagnation temperature can occur. Determination of the mass flow fluctuation level is thus rendered more difficult since the hot-wire is sensitive to both variables, and an improved technique is necessary to distinguish between them. The apparatus developed for this purpose is described and some experimental results presented to illustrate the method used to separate the two variables.

Contents

4.1/

---

1. Introduction

A previous series of turbulence and static heat loss measurements at high subsonic and supersonic speeds[1] indicated that fluctuations in stagnation temperature could occur, and their presence made mass flow fluctuation measurements more difficult. The equipment used for this work was of the constant resistance type[2]. If measurements could be made at a series of different wire temperatures it would be possible to estimate the fluctuations in the two variables, and their correlation, but the constant-resistance equipment could not readily be adapted to operate over a wide range of wire temperatures. It was therefore decided to use constant-current heating, but it was essential greatly to improve the signal-to-noise ratio normally obtained.

The techniques employed are described in Section 3, and it is shown that for the band width chosen (50 kc/s) the best possible signal-to-noise ratio has been achieved in that nearly all the electrical noise at the output is due to the hot-wire itself.

The apparatus has proved sensitive enough for free stream measurements to be made, and these are described in Section 4. In separating the two variables, it was found that a simple linear theory of heat transfer from the wire gave best agreement with experiment. It is presumed that the usual non-linear effect does not occur when heat is transferred from the wire at the rates normally associated with turbulent phenomena. It was found that the mass flow fluctuations in the test diamond of the M = 1.6 liners of the 9" × 3" induced-flow tunnel at the N.P.L. was 0.2%, and that the stagnation temperature fluctuation was 0.03%

2. The Heat Transfer Law for Hot-Wires

Recent investigations of heat transfer from hot-wires[3,4,5] indicate that the parameters are related in the following way

$$Nu = (a' + b'\sqrt{R_e})\left(1 - C\,\frac{R - R_o}{R_o}\right) f(M) \qquad \ldots.(1)$$

where $$Nu = \frac{I^2 R}{\pi \ell k \Delta T}$$

and/

and ℓ = wire length

k = conductivity of air at relevant temperature

ΔT = temperature difference

a', b', C = constants of wire

R_e = wire Reynolds number

R_o = mean temperature of wire unheated in the stream

$f(M)$ = Mach number dependent function.

An expression for $f(M)$ has been derived in (1) where it was found that

$$f(M) = \frac{\alpha + \beta M}{\gamma + \delta M}$$

so that at low Mach numbers $f(M) \to \frac{\alpha}{\gamma}$ and at high Mach numbers $f(M) \to \frac{\beta}{\delta}$.

The Mach number for the present series of tests has been chosen so that $f(M)$, and hence Nu, is insensitive to small changes in M. In this way Mach number fluctuations are not detected and the separation of mass flow and stagnation temperature fluctuations is facilitated.

The cause of the non-linear term $\left(1 - C \frac{R - R_o}{R_o}\right)$ is not yet fully understood and, as will be seen later, this term has a profound effect on the separation of the two variables from the experimental data.

2.1 The separation of mass flow and stagnation temperature fluctuations

The heat transfer equation (1) may be written

$$R = K \sqrt{R_e} (R - R_o) \left(1 - C \frac{R - R_o}{R_o}\right), \qquad \ldots\ldots(2)^+$$

and by differentiating logarithmically we obtain

$$\frac{dR}{R} = \frac{dR_o}{R_o} - \frac{\beta}{2} \frac{dR_e}{R_e} \quad \text{where} \quad \beta = x\left[\frac{1 - Cx}{1 - Cx(x + 2)}\right] \qquad \ldots\ldots(3)$$

$$x = \frac{R - R_o}{R_o}.$$

It has been shown[1,4,5] that the equilibrium temperature of the wire, T_o, is a fixed percentage of the stagnation temperature of the flow at a given Mach number, and it is reasonable to suppose that fluctuations in T_o are reflected in fluctuations in R_o; hence we have

$$\frac{dR_o}{\overline{R_o}} = \frac{dT_o}{\overline{T_o}},$$

where the bars denote mean values.

Since/

+In deriving equation (2), the a' term of equation (1) has been omitted as being negligible compared with the $b'\sqrt{R_e}$ term.

Since in practice we cannot conveniently measure instantaneous changes in resistance, but only mean square values, the mean square voltage change across the wire is measured; thus

$$\overline{\left(\frac{idR}{iR}\right)^2} \quad \text{or} \quad \overline{\left(\frac{dV}{V}\right)^2}$$

is obtained. The terms $\frac{dR_o}{R_o}$ and $\frac{dR_e}{R_e}$ are then deduced from the quadratic equation

$$\overline{\left(\frac{idR}{iR}\right)^2} = \overline{\left(\frac{dR_o}{R_o}\right)^2} + \frac{\beta^2}{4}\overline{\left(\frac{dR_e}{R_e}\right)^2} - \beta\overline{\left(\frac{dR_o}{R_o}\right)\left(\frac{dR_e}{R_e}\right)}. \quad ..(4)$$

Since there are three unknowns $\frac{dR_o}{R_o}$, $\frac{dR_e}{R_e}$ and $\overline{\frac{dR_o}{R_o}\cdot\frac{dR_e}{R_e}}$ in the quadratic, at least three values of current are required for the solution. In practice experimental scatter necessitates many more than three equations for accurate solution, and a least squares method is used to obtain the unknowns which best fit the experimental data. Alternatively it is possible to obtain the three variables by a graphical method from the data without solving the simultaneous quadratic equations. This can be done by making use of the fact that equation (4) is a quadratic in β, so that if $\overline{\left(\frac{idR}{iR}\right)^2}$ is plotted against β the result should be a parabola.

If we write $y = \overline{\left(\frac{idR}{iR}\right)^2} = a + b\frac{\beta}{2} + c\frac{\beta^2}{4}$,

where $a = \overline{\left(\frac{dR_o}{R_o}\right)^2} = \overline{\left(\frac{dT_o}{T_o}\right)^2}$

$$b = 2\overline{\left(\frac{dT_o}{T_o}\cdot\frac{dR_e}{R_e}\right)}$$

$$c = \overline{\left(\frac{dR_e}{R_e}\right)^2}$$

we obtain, by completing the square

$$y = c\left[\frac{\beta}{2} + \frac{b}{2c}\right]^2 + \left[a - \frac{b^2}{4c}\right],$$

so that the vertex of the parabola is at the point

$$\beta_v = -\frac{b}{c} \qquad y_v = a - \frac{b^2}{4c}.$$

Now a is given by the value of y, say y_o, when $\beta = 0$ so that

$$\frac{b^2}{4c} = y_o - y_v$$

and/

and $$\frac{b}{c} = -2\beta_v,$$

hence $$c = \frac{y_o - y_v}{\beta_v^2}.$$

The correlation coefficient is defined to be

$$\frac{\frac{dR_e}{\overline{R_e}} \cdot \frac{dT_o}{\overline{T_o}}}{\sqrt{\left(\frac{dR_e}{\overline{R_e}}\right)^2}\sqrt{\left(\frac{dT_o}{\overline{T_o}}\right)^2}} = \frac{b}{2\sqrt{ac}} = \left(1 - \frac{y_v}{y_o}\right)^{\frac{1}{2}}.$$

In Fig.1, y is plotted as a function of β with equal dR_e and dT_o, but with the correlation coefficient as a variable. Fig.2 is a plot of the value of y for a correlation coefficient of -0.5, with $dT_o/\overline{T}_o = 0.2\ dR_e/\overline{R}_e$. Since in practice there is a limit of about 0.5 to β, it is fortunate that generally one variable is many times the other so that the parabola is well defined by a few points.

3. Equipment

A brief description of the electronic techniques involved is given. Apart from noise considerations there is nothing unusual in the design.

3.1 Noise considerations in the amplifier

The ultimate sensitivity of any electronic amplifying apparatus is reached when the random thermal agitation of electrons in resistors and valves produces a voltage which, referred to the input terminals, is of the same order of magnitude as the signal. Since the output of a hot-wire anemometer in a turbulent flow is random, and not unlike that from thermal noise which typically has a uniform spectral density, the problem of distinguishing signal and noise is even more difficult than usual. Generally the lowest signal level needs to be at least twice the noise level if adequate resolution is to be achieved.

The noise current in a valve can be expressed most conveniently by assuming a perfect noise-free valve, and attributing all the internal noise to an external resistance, the "equivalent noise resistance" R_{eq}, and the noise voltage E_N across the resistance is given by

$$E_N = \sqrt{4\,k\,T R\,df} \text{ volts},$$

where

k = Boltzmann's constant 1.38×10^{-23}

T = absolute temperature of R

R = resistance R_{eq} in ohms

df = band width, cycles/second.

Typical values for R_{eq} are given in Table I, where it will be seen that triodes have typically lower R_{eq}'s than pentodes. Despite the

improvement/

improvement possible with the use of triodes, the noise produced by a single triode (R_{eq} = 400 ohms) with a band width of 50 kc/s is 0.58μv, whereas the noise signal from the hot-wire of say 4 ohms resistance is only 0.058 μv. It is seen that the valve produces far more noise than the wire. Some reduction in noise contribution from the valve result from the use of two or more values in parallel. For two equal valves in parallel, it can be shown that the equivalent noise resistance is $R_{eq}/2$, and the signal to noise ratio is improved by a factor of $\sqrt{2}$.

If, however, we insert a transformer between the wire and the valve, Fig.3, it is possible to obtain an impedance multiplication of n^2 where n is the turns ratio of the transformer. The wire resistance and resistance variations now appear as n^2R_w and $n^2\Delta R_w$ at the grid of the valve, and it is quite feasible to make $n^2R_w >> R_{eq}$. The wire itself is now the major source of noise, and the ultimate resolution of the equipment is determined by the wire. This represents the best which can be done with the hot-wire as a sensing element.

It is necessary for the transformer to have a wide frequency range and uniform response, and it is probably this fact which has prevented its use in the past. Transformers are now available with impedance transformations of 3 ohms to 6000 ohms with level response from 40 c/s to 100 kc/s, and thus for a 4 ohm wire resistance the reflected resistance is 15 times that of the valve. To achieve the widest possible band width it is necessary to terminate the transformer with its characteristic impedance, but there is no serious loss at low frequencies if this is omitted. The transformer used had the following characteristics

Primary Inductance	(3Ω winding)	3 mH
Secondary "	(6000Ω winding)	18 H
Mutual "		360 mH.

3.2 Noise amplification in the compensator

Since the signal at the hot-wire falls uniformly at 6dB/octave after a frequency given by $f = \frac{1}{2\pi\tau}$, where τ is the wire time constant, an amplification which rises with frequency must be provided, and this stage amplifies noise and signal without discrimination. If the overall band width is extended sufficiently, a limit will be reached at which noise from the wire predominates and no further information can be obtained by extending the band width. The noise from the first valve in the amplifier or from the wire itself may be written as an equivalent input

$$E_N^2 = 4\,k\,T\,R\,df,$$

and if $\tau = \frac{1}{2\pi f_1}$, where f_1 is the frequency at which the compensator gain begins to rise, E_N may be expressed in the form

$$\frac{E_{NO}^2}{G_o^2} = [1 + (2\pi)^2 f^2 \tau^2]\, 4\,k\,T\,R\,df$$

where G_o = overall gain of system at frequencies $<< f_1$

and E_{NO} = noise voltage at output R.M.S.

The/

The total noise between any limits f_2 and f_3 is given by

$$\frac{E_{NO}^2}{G_O^2} = \int_{f_2}^{f_3} 4\,k\,T\,R\,[1 + (2\pi)^2\,f^2\,\tau^2]\,df$$

$$= 4\,k\,T\,R\,(f_3 - f_2) + \frac{16}{3}\,\pi^2\,\tau^2\,k\,T\,R\,(f_3^3 - f_2^3).$$

For $f_3 >> f_2$, which is the usual case,

$$\frac{E_{NO}^2}{G_O^2} = \frac{16}{3}\,\pi^2\,\tau^2\,k\,T\,R\,f_3^3 \quad .$$

This function has been plotted in Fig.4 for various values of R and τ.

Several circuits have been suggested for achieving the requisite frequency characteristic for compensation[6,7,8]. The one chosen is similar to that described in (8), being a negative feedback system with a time constant equal to the wire time constant in the feedback loop. Compensation can be achieved at least up to 100 kc/s. The circuit is given in Fig.5 with response curves for various compensation settings in Fig.6. Without some prior knowledge of the fluctuation levels and wire sensitivities, it is impossible to arrive at a rational value for the upper frequency limit. Clearly a filter must be placed after the compensator since the gain of this unit is rising steadily, and in practice it was found that the output stages were overloaded by input noise alone unless a filter was used. The type of flow to be investigated also has a bearing on the selected cut-off frequency. In typical isotropic free streams the spectrum decays, whilst in boundary-layer flows there is evidence of frequencies above 100 kc/s. Since the present equipment was primarily intended for use in the free stream, the band width was put tentatively at 50 kc/s to give a spatial resolution of 0.01 ft at 1000 ft/sec. A sharp cut-off filter was inserted after the compensator unit. The compensator is linear to 100 kc/s, and it would be a simple matter to substitute a 100 kc/s filter if desired.

Since the equivalent noise input E_{NO}/G_O is a function of the compensation setting, it is possible to check the operation of the input stage and compensator. A wire of 6.5 ohms cold resistance was connected across the input transformer through a 6000 μF condenser, and its temperature raised to 488°K at which temperature its resistance was 11.64 ohms. Readings of R.M.S. output noise were then taken as the compensation setting was altered, and the equivalent input values plotted against τ. The results are presented in Fig.7, and it will be seen that fair agreement with the theoretical straight line is achieved.

3.3 The output stages

The output of the filter is a random signal, and to obtain steady meter readings this signal is fed via a cathode follower to a vacuo-junction. A range of series resistances enables a suitably large deflection to be obtained on the millivoltmeter, and a calibration curve is used to convert this reading to equivalent input with the compensation off.

3.4/

3.4 Measurement of wire time constant

Since the input transformer is attached directly to the wire for noise reduction, the usual method of injecting a large audio-frequency signal at the bridge input, Fig.8, will not suffice since an output would result at all frequencies independently of wire time-lag effects. If, however, a modulated radio-frequency carrier is injected at the wire terminals, this difficulty is overcome. The carrier is a convenient method of adding heat to the wire at a determined frequency, and no output response is obtained from the mean carrier level since the carrier frequency can be chosen well above the cut-off frequency of the equipment. A crystal controlled oscillator and screen grid modulated amplifier operating at 5.5 Mc/s were used. The essential features of this system are shown in Fig.9, with a typical wire response curve with and without compensation in Fig.6. Instead of plotting a complete wire response curve to determine the time constant, it was found easier in practice to switch the modulation frequency from some value below $w = 1/\tau$, say 100 c/s, to one well above 1000 c/s, and adjust the compensation until the two outputs were equal within the limits of 0.01 milliseconds allowed by the compensator circuit.

Since frequencies below $f = 2U/\lambda$, where U is the mean tunnel speed and λ the length of the working section, should be ascribed to fluctuations in mean tunnel speed, f represents the lowest frequency at which turbulence measurements are valid. In the present series of experiments f was about 1200 c/s. Thus frequencies below the break point of the wire are of no interest, and all that is needed is any one rising compensation characteristics. It is still necessary to determine the wire time constant, however, in order to know the overall gain at frequencies below the break point since an error in τ will produce an error in the overall gain.

3.5 Wire power unit

It is convenient to use the anode circuit of a medium power valve to maintain a constant current in the hot-wire, since grid control enables the current to be varied within fine limits. The principle is illustrated in Fig.8. A large electrolytic condenser is connected between the grid and ground to present zero impedance for noise suppression. A well regulated power supply for the value is still essential.

3.6 Hot-wire probe

It is important in high-speed flows that the hot-wire be upstream of any disturbances created by the supports. Despite this, all measurements relate to the flow behind the shock from the wire itself. For this reason the original spot welding technique[9] has been abandoned in favour of copper plating the wire and soft soldering. The bath for selectively plating the wire is shown in Fig.10. A current of 1 mA deposits 5 to 10 wire diameters on the tungsten in 10 to 20 minutes. A pure cu SO_4 bath, 250 gm to 1000 ml, is used and a fine resin core solder (34 S.W.G.) for soft soldering to the needle support (Fig.11). Such probes were found entirely satisfactory for the present investigation, and all the results described in later sections were obtained with one wire which ran for over 30 hours at M = 1.6. Tungsten wire of 0.00025 inch diameter has been found most suitable.

4. Turbulence Measurements

In Section 2 it has been noted that the heat transfer function is independent of Mach number at both high and low Mach numbers. M = 1.6 was chosen as being sufficiently beyond the range where Mach number variations are significant.

4.1/

4.1 Measurements in the free stream at M = 1.6

The probe was located centrally in the test diamond, and the wire resistance varied from 3.775 to 5.132 ohms. The value of x (Equation (3)) thus ranged from 0.06 to 0.44. It was not possible to obtain x values larger than 0.50 without oxidising the tungsten wire, and altering the calibration. The desired resistance was set on the wheatstone bridge (Fig.8), and the bridge current increased until balance was obtained. The mean wire voltage was then determined by means of a potentiometer, and the time average of the fluctuating wire voltage squared by the vacuo-junction as already described.

The equilibrium wire resistance R_o is most readily found by extrapolating wire power input to zero (Fig.12), and C, the non-linear term, from the relationship

$$C = \frac{W_2 x_1 - W_1 x_2}{W_2 x_1^2 - W_1 x_2^2}$$

where $$x = \frac{R - R_o}{R_o}$$

W_1 = power at $x = x_1$

W_2 = power at $x = x_2$.

From the smoothed curve in Fig.13 for the wire used, a value of 0.5 is obtained for C. If now the term $\left(\frac{\overline{idR}}{iR}\right)^2$ is plotted directly against $\frac{R - R_o}{R_o} = x$ without correction for the non-linear heat transfer term in equation (1), the curve (1) in Fig.14 results and the least squares parabolic equation of the form $y = a + \frac{bx}{2} + \frac{cx^2}{4}$ is curve (2) in Fig.14.

Applying the correction $\frac{1 - Cx}{1 - Cx(x + 2)}$ to the overheating ratio, curve (3) is obtained which has a point of inflection and cannot be approximated by a parabolic equation. The correction factor has been plotted in Fig.15 for values of C from 0.1 to 0.6. It will be seen that for C as found statically x tends to ∞ for $C = \frac{R_o^2}{R^2 - R_o^2}$, and $\left(\frac{\overline{idR}}{iR}\right)^2$ approaches an horizontal asymptote.

Apparently best agreement with experiment demands that we neglect the effect of non-linear heat transfer.

Any attempt to explain this phenomenon must remain tentative until the mechanism of heat transfer from the wire is more fully understood. Alternatively it is possible that another type of fluctuation besides mass flow and stagnation temperature invalidates the choice of a quadratic equation. One such variable is the sound wave mode, but this has been shown[10] to have an increasing linear effect with x, and the presence of sound waves could not account for the inflection observed nor the departure from parabolic form at the vertex.

A/

A second explanation is that the value of C obtained from steady state measurements does not apply under dynamic conditions where heat is transferred from wire to stream at rates up to 50 kc/s. If the non-linear term were caused by some redistribution of the velocity field around the wire, then it is not unreasonable to suppose that this distribution would not change at the same rate as the heat transfer phenomena. Hence two different values of C are needed, and it appears from the experimental data that C = 0 is the best compromise for dynamic purposes.

This being the case, we may obtain by a least squares method the best fit parabola

$$y = \overline{\left(\frac{idR}{\bar{iR}}\right)^2} = 1.6 - 11.84\left(\frac{x}{2}\right) + 117\left(\frac{x}{2}\right)^2$$

where $$x = \frac{R - R_o}{R_o}.$$

Thus if G_o is the gain of the amplifier up to the filter unit at which idR is found equal to 2720,

$$\frac{dR_e}{\bar{R_e}} = \frac{\sqrt{117} \times 100}{2720}$$

$$= 0.29\%$$

and

$$\frac{dT_o}{\bar{T_o}} = \frac{\sqrt{1.6} \times 100}{2720}$$

$$= 0.034\%.$$

4.2 Measurements behind a plane inclined shock

In order to examine the separation process where one variable is not much greater than another, the probe was placed behind the attached shock wave of a double wedge aerofoil section (Fig.16), and the same technique was used to determine $dR_e/\bar{R_e}$ and $dT_o/\bar{T_o}$. In Fig.17 $y = \overline{(idR/\bar{iR})^2}$ is again plotted against x, and comparison with Fig.14 shows that the parabola is now flatter and the vertex has moved in the direction of increasing x.

The least squares solution for C = 0 is

$$y = 0.8345 - 0.32\left(\frac{x}{2}\right) + 2.656\left(\frac{x}{2}\right)^2$$

with the gain between wire and filter now 1675 so that

$$\frac{dR_e}{\bar{R_e}} = 0.12\%$$

and

$$\frac{dT_o}{T_o} = 0.06\%.$$

The/

The interchange of energy from ΔR_e to ΔT_o has reduced the difference between them, and the parabola is more like (2) in Fig.2 while the previous case, the free stream flow, corresponded to curve (1) in Fig.2.

4.3 Measurements in the turbulent boundary layer on the tunnel wall

A series of fluctuation measurements was made at stations 0.1, 0.3, 0.5, 0.7, 0.9 and 1.1 cm from the lower wall of the nominal M = 1.6 liner. Some initial difficulty was experienced due to the high signal level, but this was overcome by removing the input transformer and connecting the wire directly to the grid of the first amplifier through a large condenser. The results obtained at the first station d = 0.1 cm are plotted in the usual manner in Fig.18. Since a least squares solution at each station would have been a tedious procedure, the method of "selected points"[11] was used to obtain the parabolic equation. The levels of $dR_o/\overline{R_e}$, $dT_o/\overline{T_o}$ and the correlation coefficients for the six stations are shown in Fig.19. The signal at distances greater than 1.1 cm from the wall was of the intermittent turbulent type indicating the uneven edge of the boundary layer, and no turbulence measurements were made in this region. The profile, for this limited range at least, is similar to that reported by Kovásznay[12], although the temperature fluctuations observed in the present work are much less than in Ref.12.

The experimental points fit as closely as can be expected to the parabolic form, and it is concluded that the two dominant fluctuation modes are mass flow and stagnation temperature, although it had been anticipated that the sound wave mode would be apparent. Attempts to obtain the diagram for a pure sound wave mode were made by placing the wire on an oscillating shock wave but the wire failed, presumably due to fatigue.

4.4 Effect of damping screens placed upstream of the tunnel contraction

Normally the tunnel is operated with two 100 mesh and one 30 mesh gauze in the contraction. Two tests were made to examine the effect of these on the turbulence level in the test diamond at M = 1.6, and it was concluded that within the limits of accuracy of the experiment there was no change when only one 100 mesh gauze was used.

5. Conclusion

The equipment as designed is suitable for free stream turbulence measurements in supersonic tunnels, and the technique suggested for differentiating between the two predominant fluctuation modes is reasonably satisfactory. A possible discrepancy between static and dynamic heat transfer conditions is noted.

6. Acknowledgments

The equipment was developed at Oxford University where one author (D.L.S.) held a Pressed Steel Research Fellowship. The co-operation of the National Physical Laboratory in providing wind tunnel facilities and the permission of the Director to publish the results is gratefully acknowledged.

References/

References

No.	Author(s)	Title, etc.
1	B. Wise and D. L. Schultz	The hot-wire anemometer for turbulence measurements. Part IV. Communicated by Prof. A. Thom. C.P. 276. April, 1954.
2	B. Wise and D. L. Schultz	The hot-wire anemometer for turbulence measurements. Part III. Communicated by Prof. A. Thom. C.P. 275. March, 1954.
3	W. G. Spangenberg	Heat-loss characteristics of hot-wire anemometers at various densities in transonic and supersonic flow. N.A.C.A. T.N. 3381.
4	H. A. Stine H.T.F.M.I., Univ. of Calif.	Investigation of heat transfer from hot-wires in the transonic speed range. June 1954.
5	L. S. G. Kovásznay and S. I. A. Törmark	Heat loss of wires in supersonic flow. Bumblebee Series. Report No.127.
6	R. W. F. Gould	A circuit for compensating hot wires used in the measurement of turbulence. R.& M.2240. (August, 1945).
7	H. Schuh	Measurement of very little fluctuations of wind (wind tunnel turbulence). MAP-VG32-80T. A.R.C. 9837. (1st May, 1946).
8	L. S. G. Kovásznay	The development of turbulence measuring equipment. N.A.C.A. T.N. 2839.
9	D. L. Schultz	The design and construction of hot-wire anemometers for high speed flows. O.U.E.L. 68. Communicated by Prof. A. Thom. A.R.C. 16,635. (4th March, 1954).
10	L. S. G. Kovásznay	Turbulence in supersonic flow. IAS 21st Annual Meeting January 26, 1953.
11	Worthing and Geffner	Treatment of experimental data. Wiley, October 1950.
12		Project SQUID. Semi Annual Report, October 1, 1952.

TABLE I/

FIGS. 1, 2 & 3

FIG 1

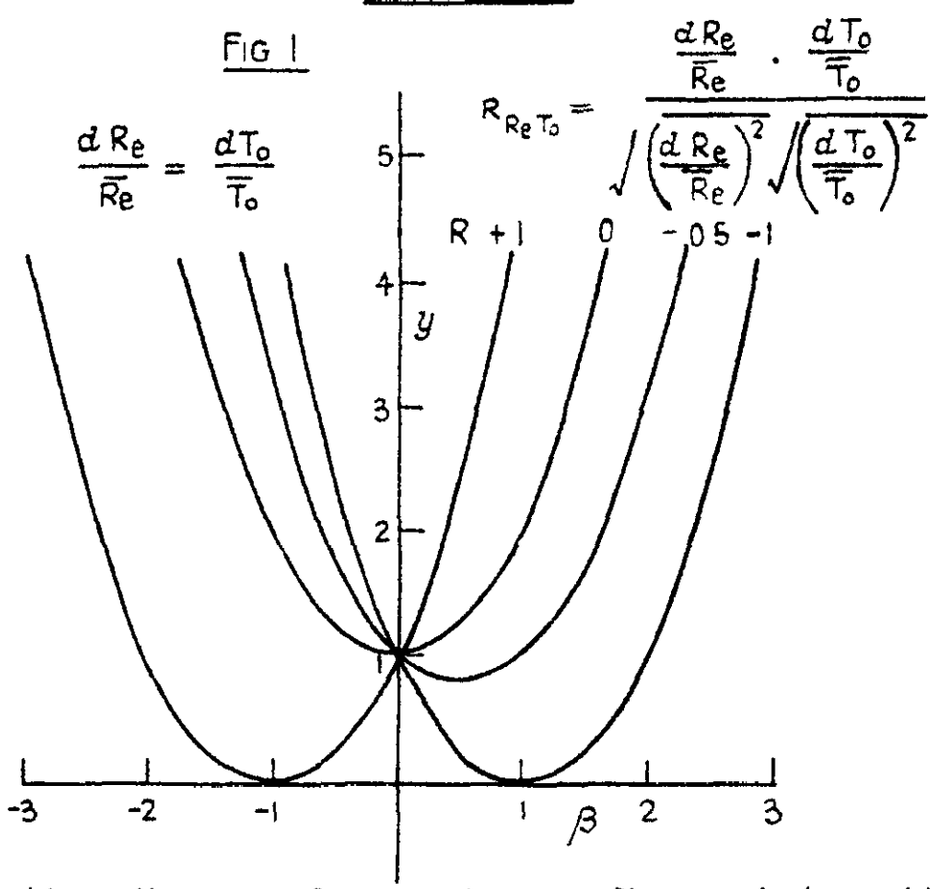

Fluctuation diagram for equal mass flow and stagnation temperature fluctuations. Correlation variable

FIG 2

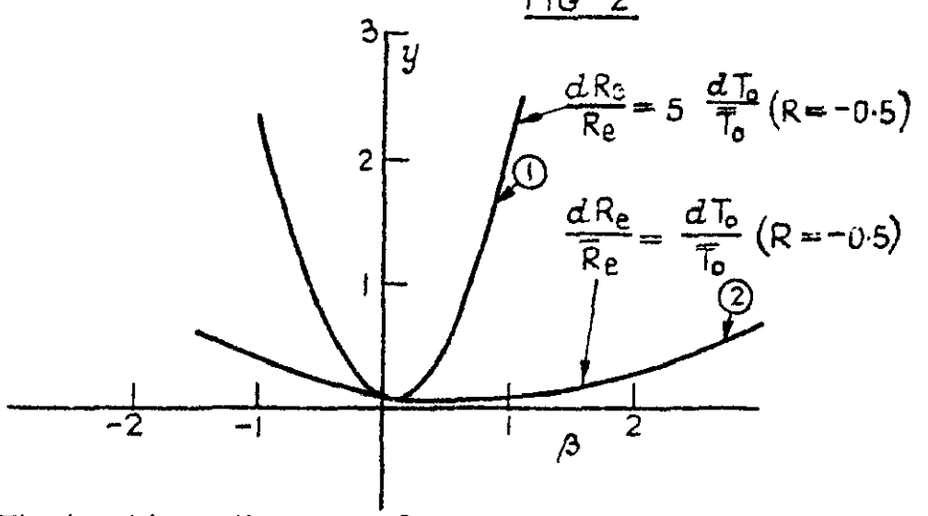

Fluctuation diagram for unequal mass flow and stagnation temperature fluctuations. Constant correlation

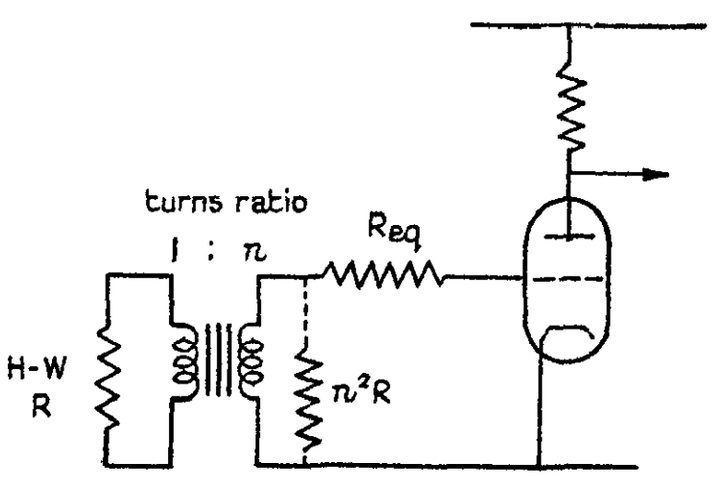

FIG. 3

The input matching circuit

FIG. 4.

$$\frac{E_{NO}^2}{G_o^2} = \frac{16}{3}\pi^2\tau^2 \; K\,T\,R \; f_3^3$$

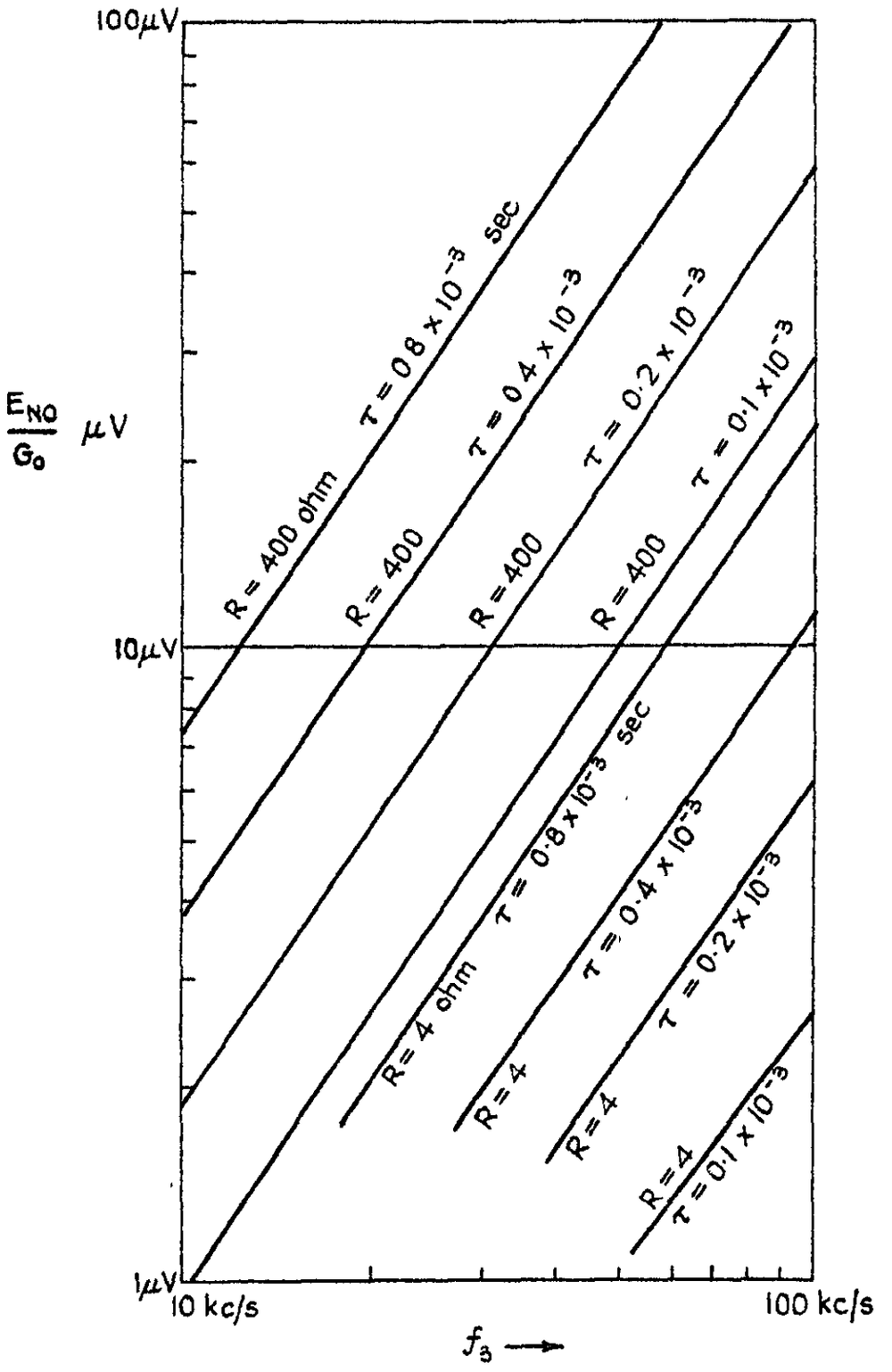

The equivalent noise input as a function of wire time constant and upper cut-off frequency.

TABLE I

Comparison of Equivalent Noise Resistances

Type	Application	g_m mho	Noise Equiv. Resist Calc.	Noise Equiv. Resist Meas.
6SK7	Pentode	2000	10,500	9 - 11,500
6AC7	"	9000	720	600 - 760
956	"	1800	9400	-
6J5	Triode	2600	960	1250
6AC7	"	11,200	220	-
6J4	"	12,000	210	-
EF50	Pentode	6,000	-	1400
EC91	Triode	8,500	-	400

ES

FIG. 5.

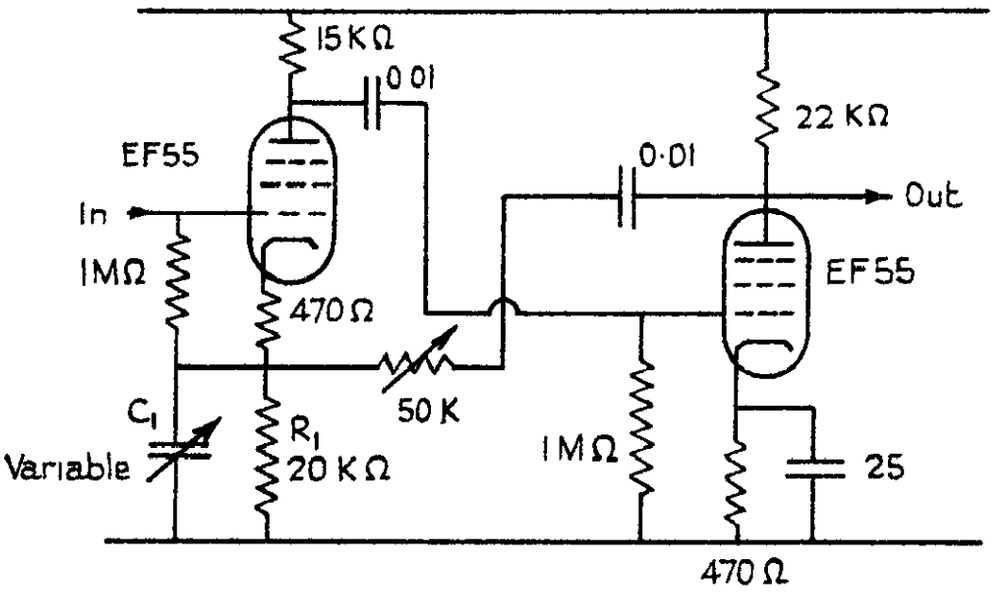

C in μF

$R_1 C_1 = \tau$ the desired time constant

The compensator circuit

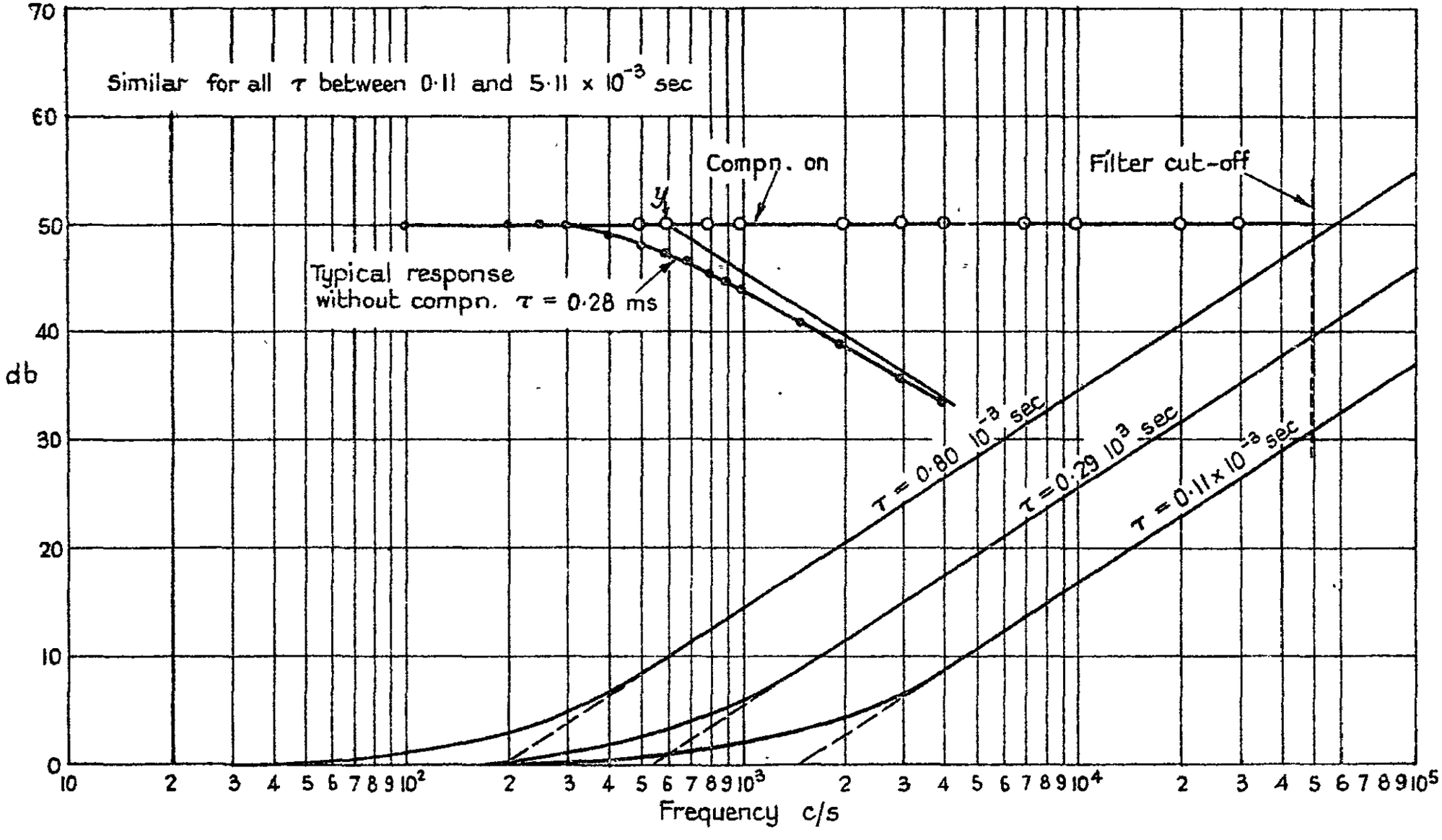

FIG. 6.

The compensator response and measurement of wire time constant τ

Fig 7

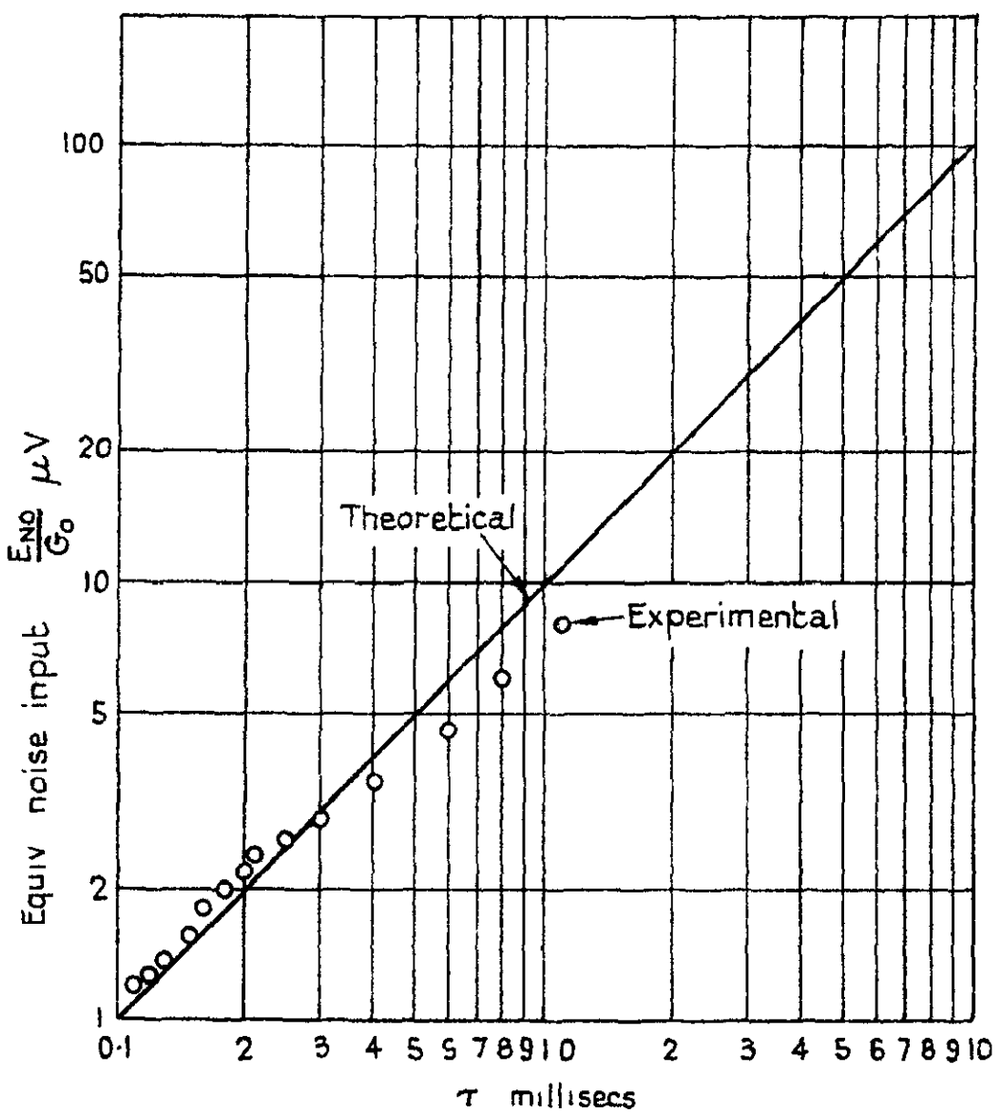

The equivalent noise input as a function of compensator setting.

FIGS 8 & 9

FIG. 8

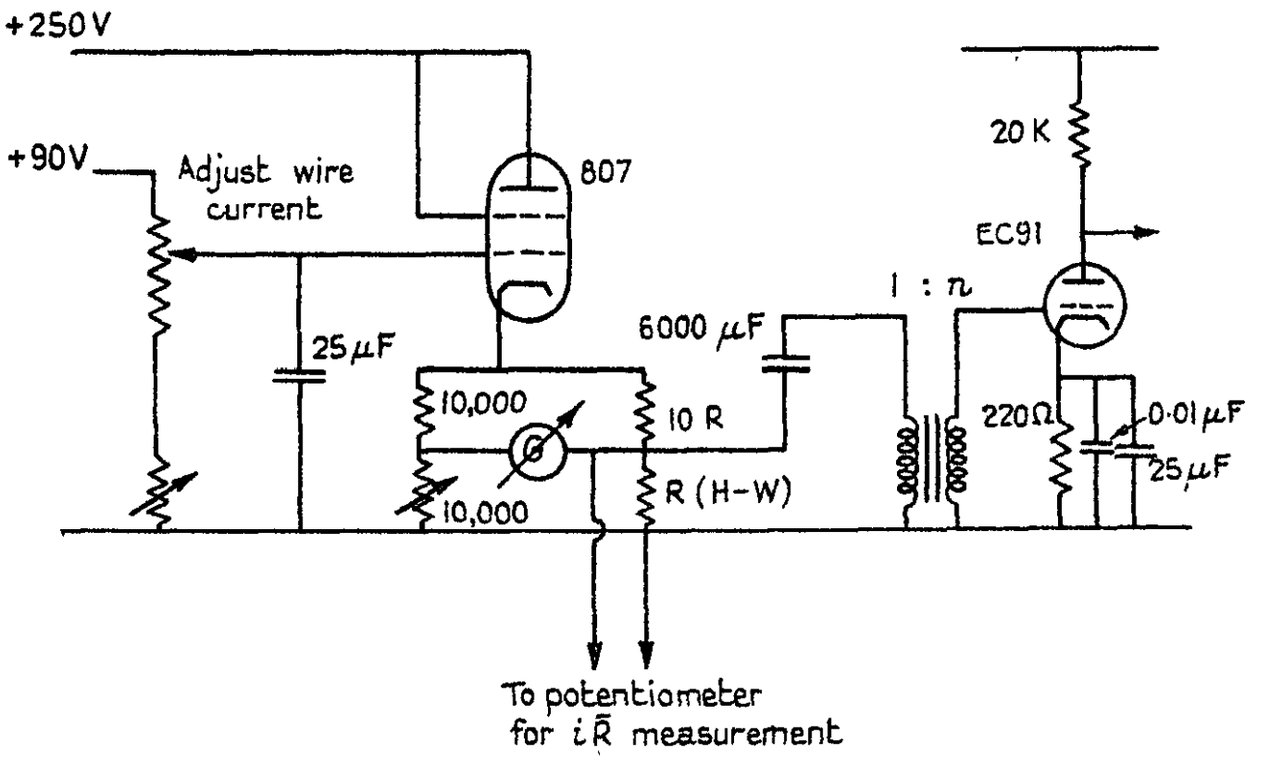

The wire heating circuit

FIG. 9.

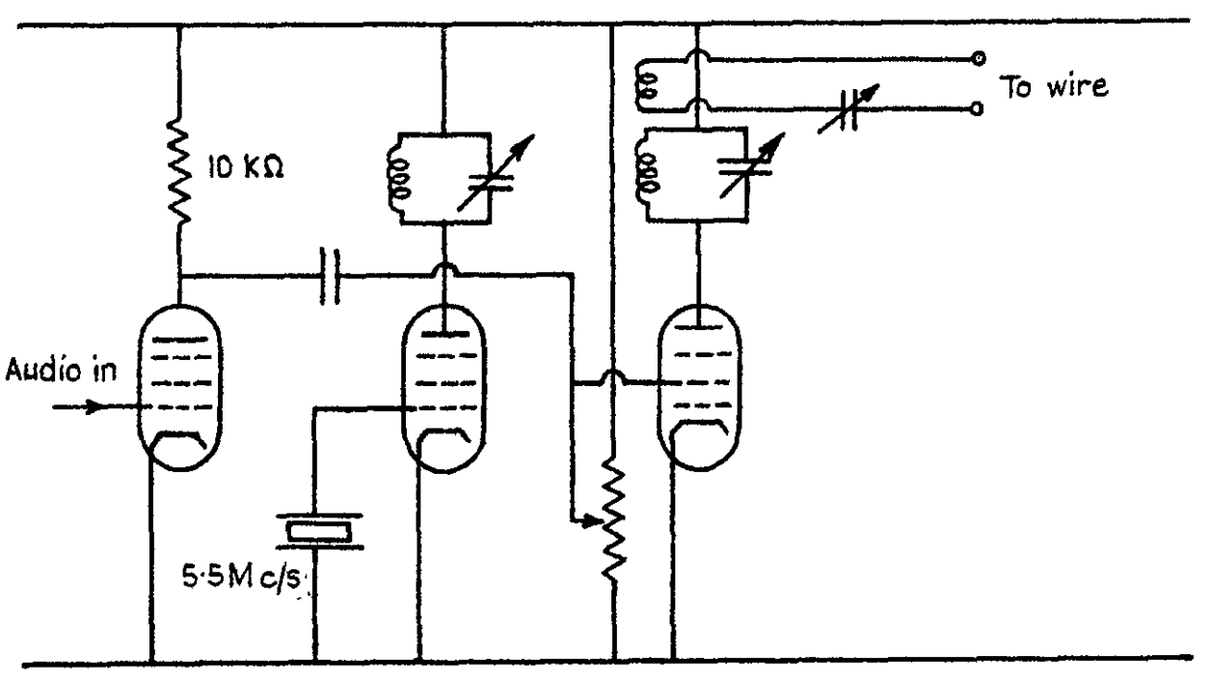

The modulated oscillator for wire time constant determination

FIGS 10 & 11

FIG. 10

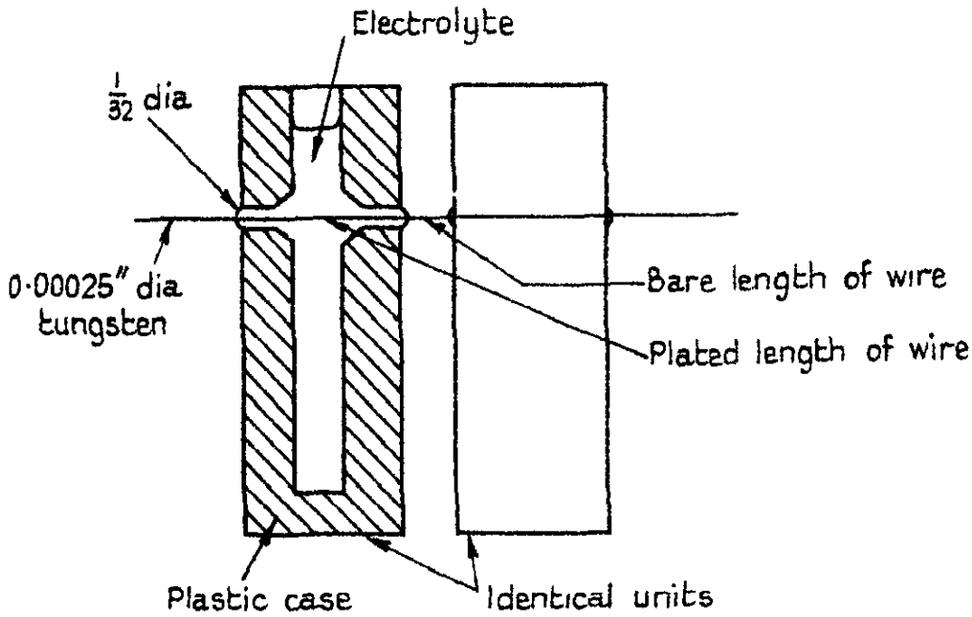

The plating bath

FIG. 11.

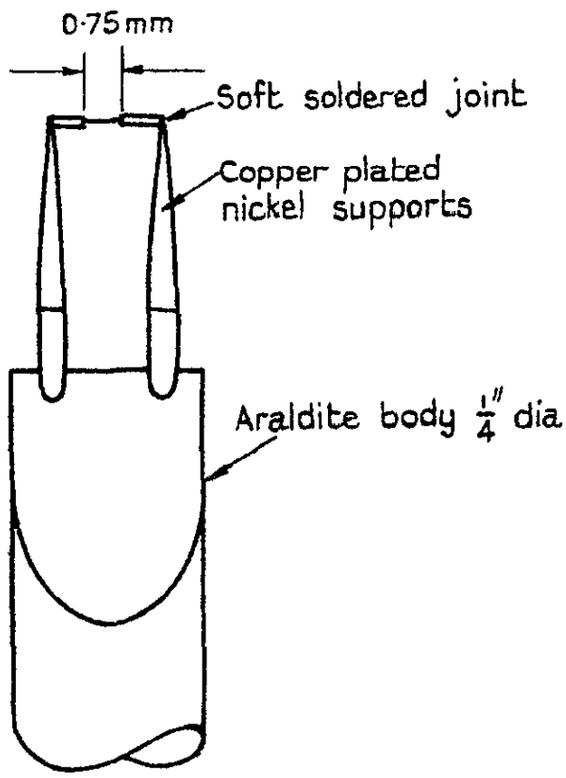

The hot-wire probe

FIG. 12.

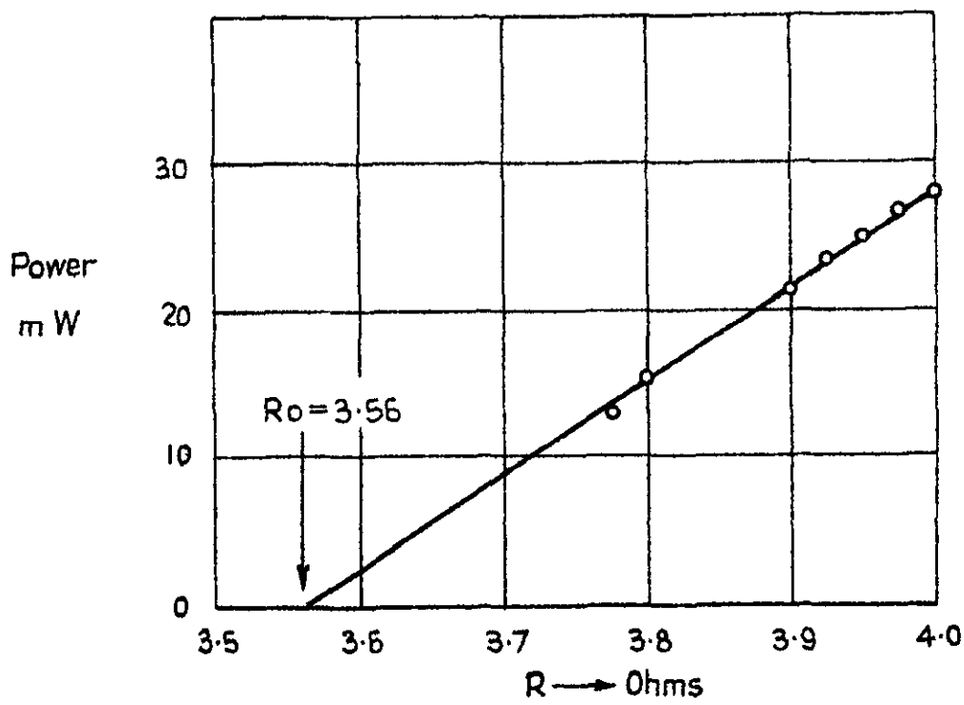

Determination of equilibrium resistance

FIG. 13.

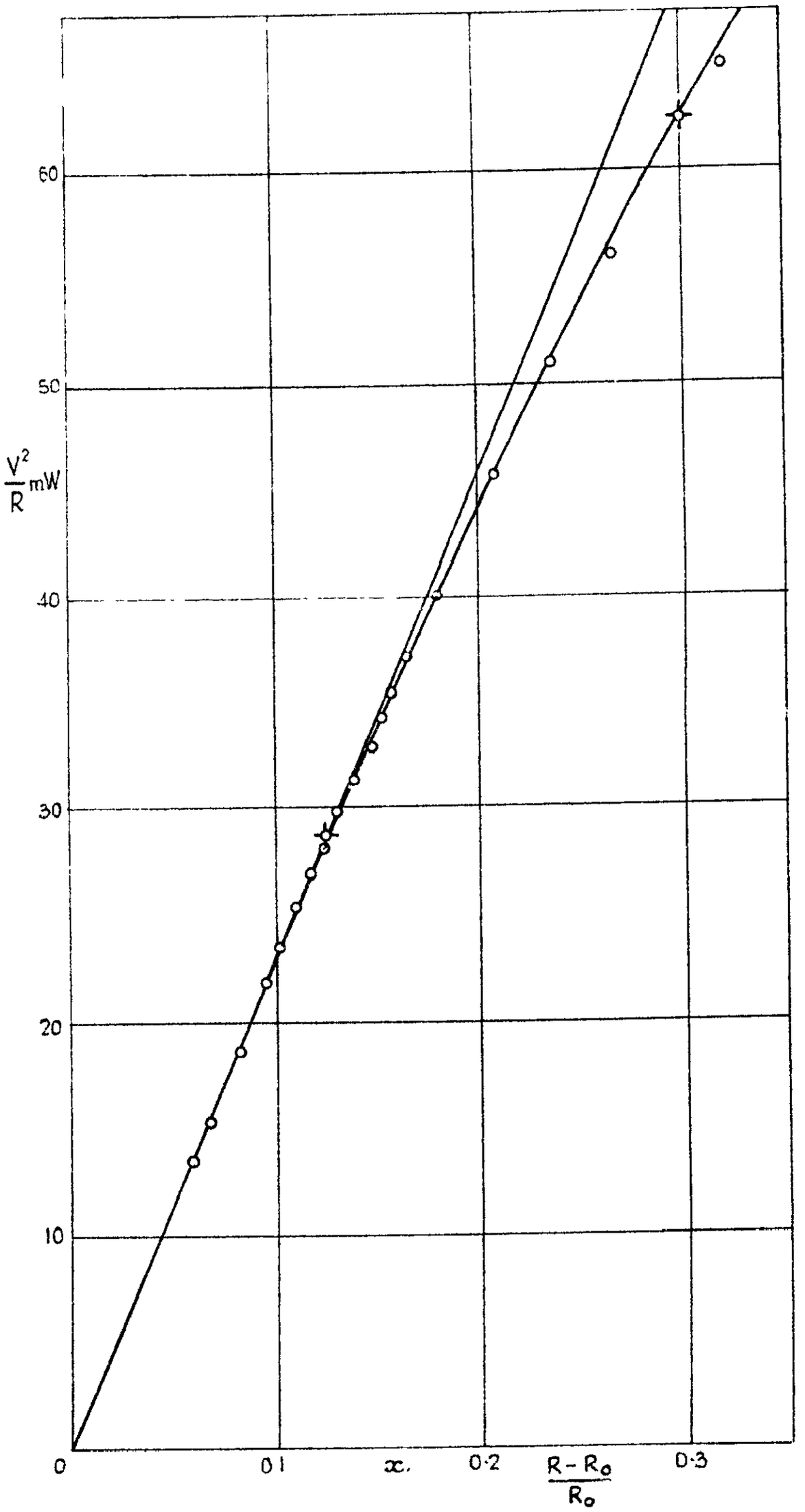

Non-linear heat transfer free stream M = 1·6 C = 0·50.

FIG. 14.

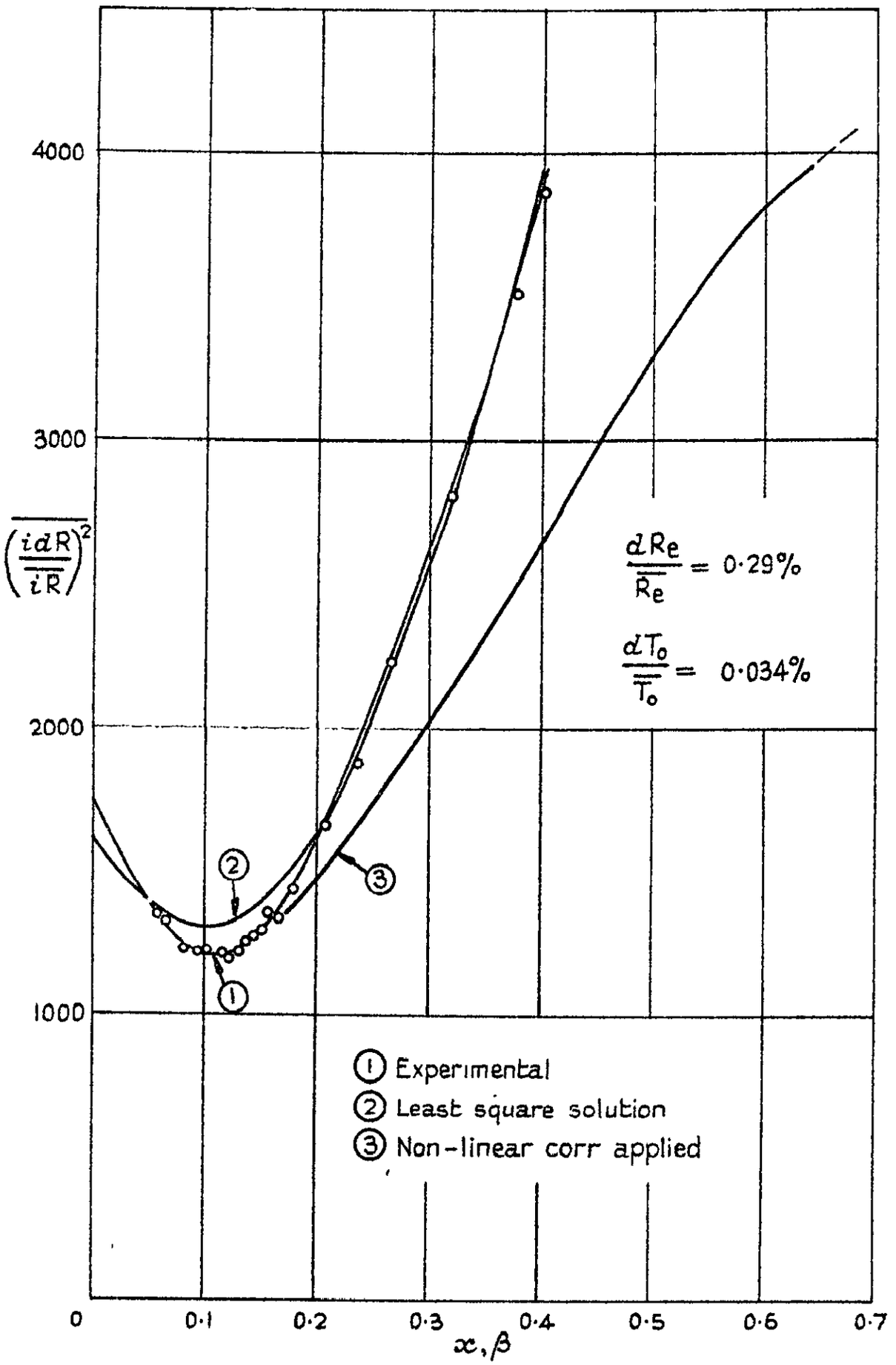

Fluctuation diagram for the free stream M = 1·6.

FIG. 15.

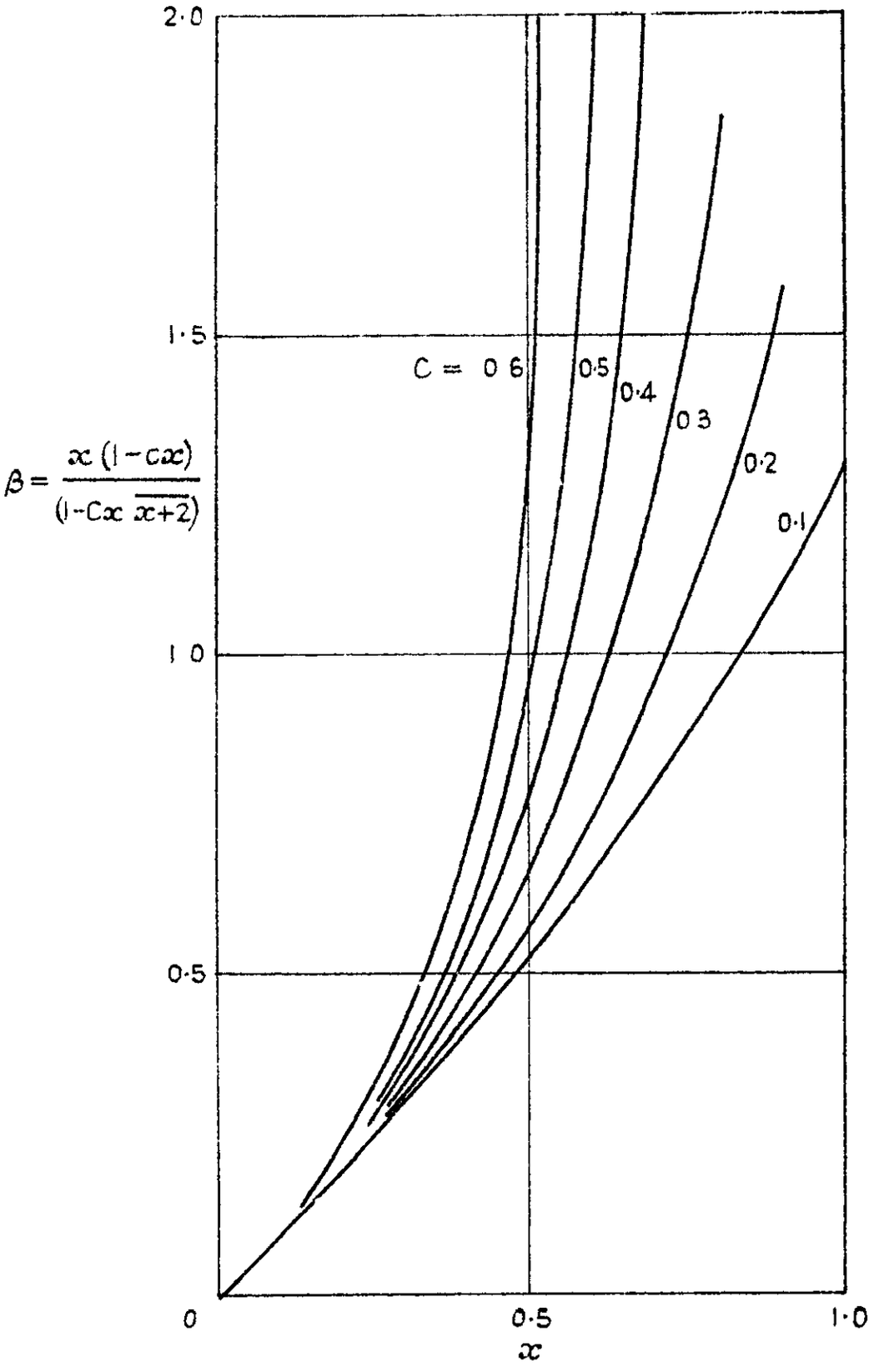

The non-linear heat transfer correction factor β

FIGS 16 & 17

FIG 16.

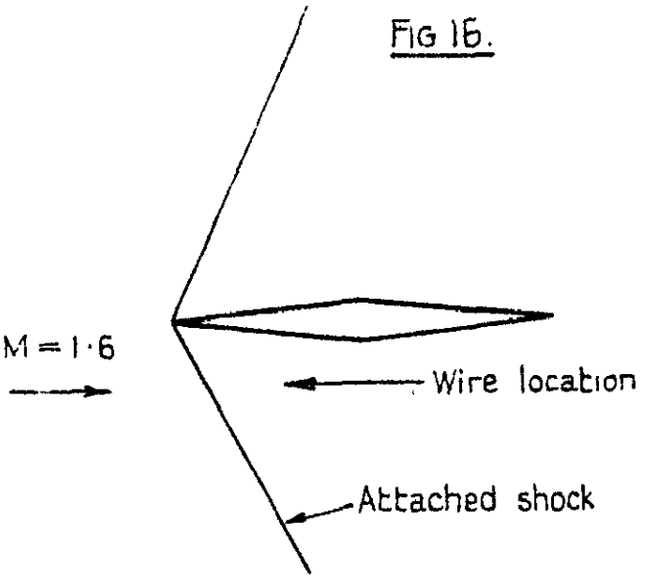

Location of the hot-wire behind a plane, inclined shock.

FIG. 17.

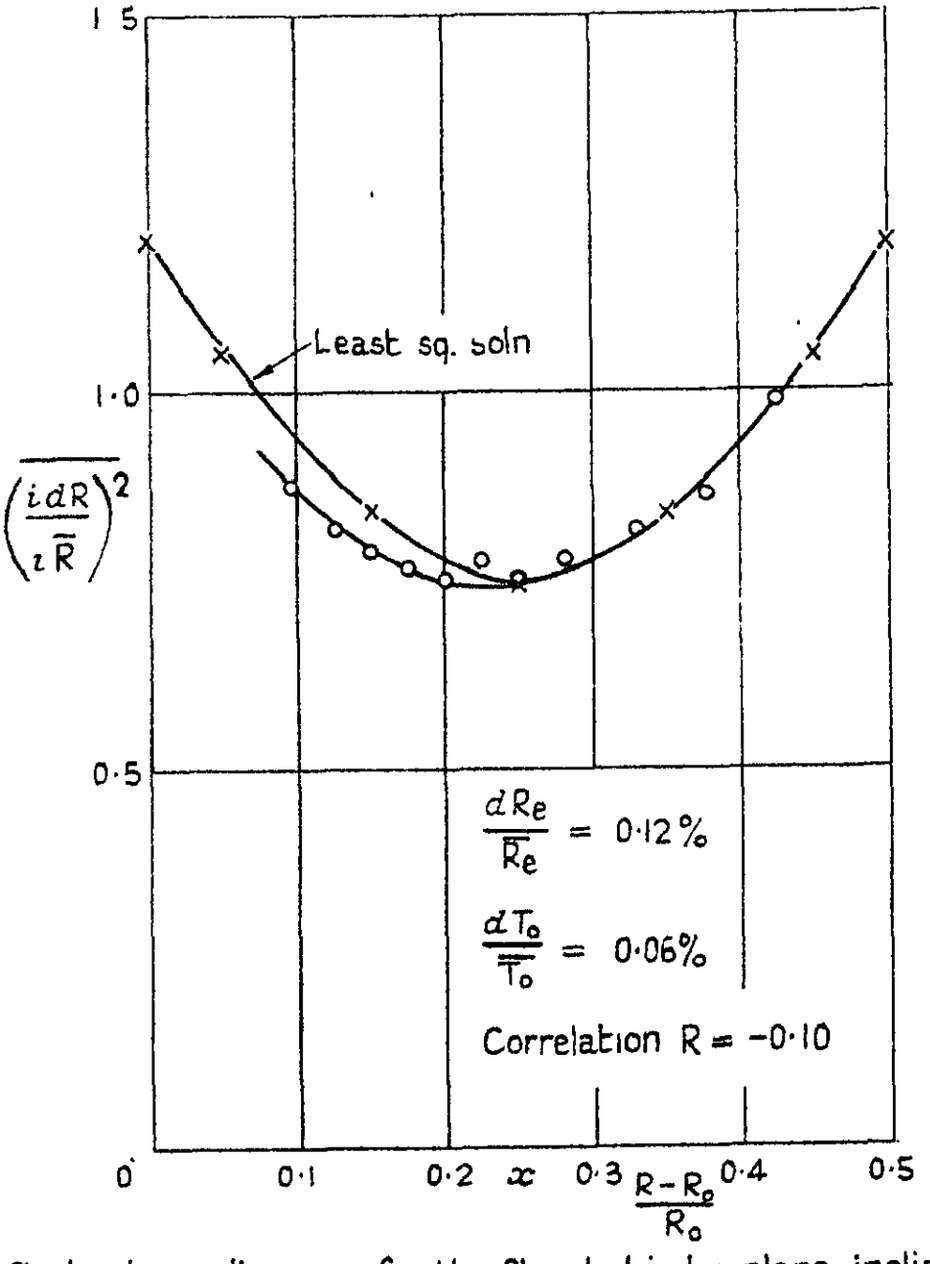

The fluctuation diagram for the flow behind a plane, inclined shock

FIG. 18.

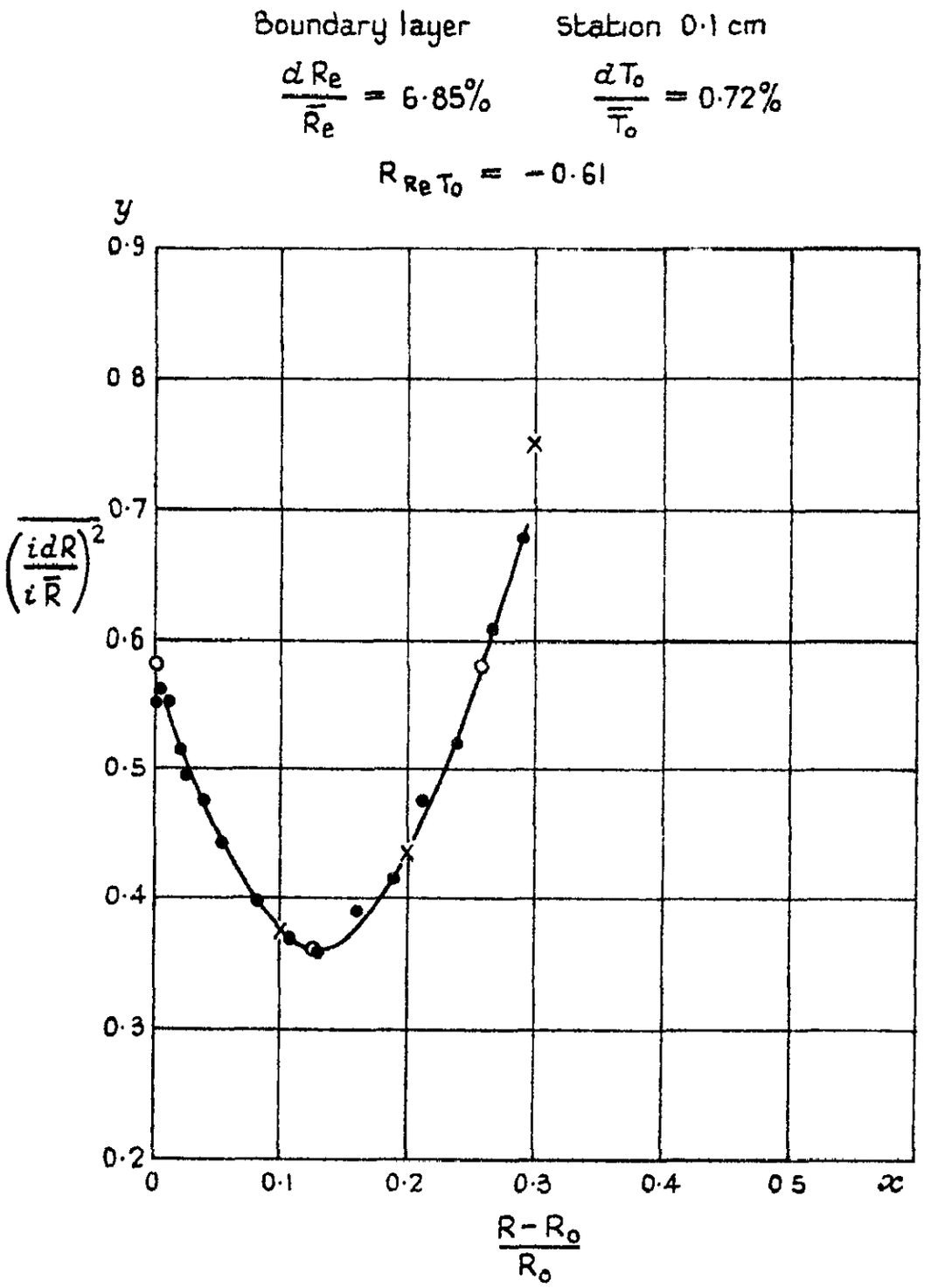

A typical fluctuation diagram for the flow in a turbulent boundary layer.

FIG. 19

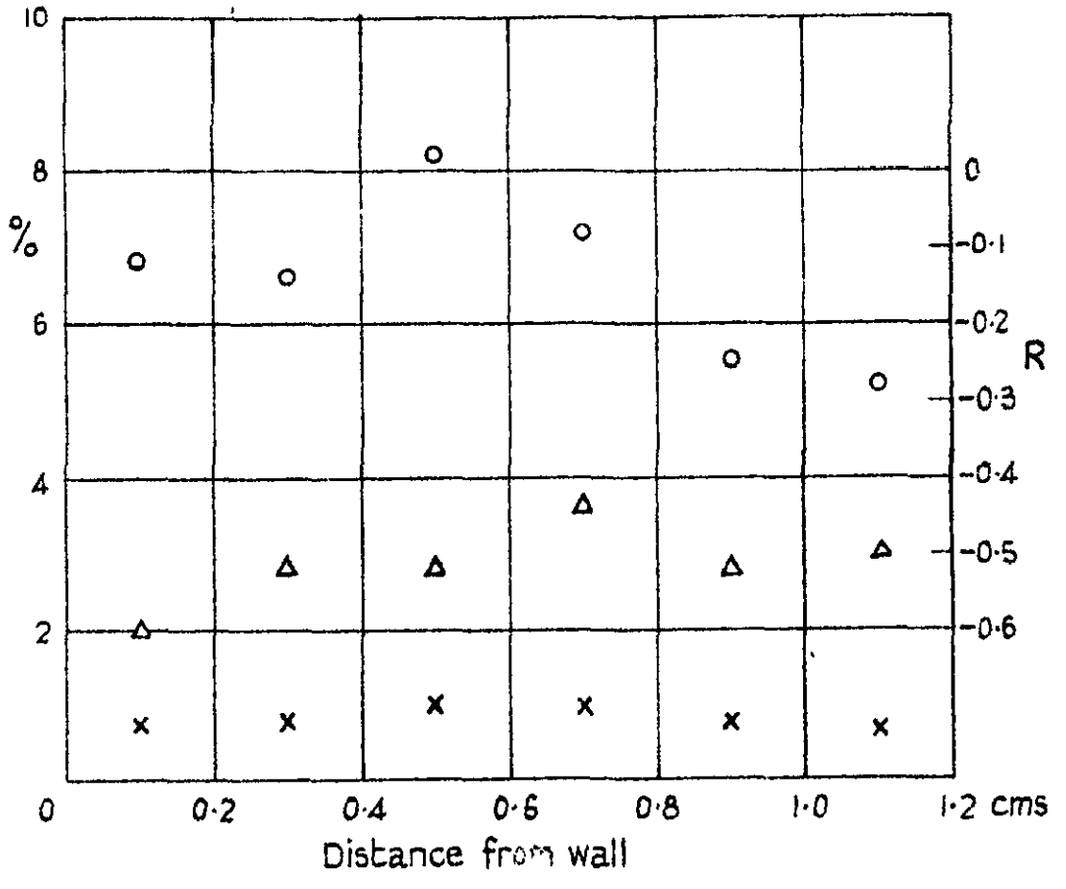

○ $\frac{d R_e}{\overline{R_e}}$ %

× $\frac{d T_o}{\overline{T_o}}$ %

△ correlation

Mass flow and stagnation temperature fluctuations in a turbulent boundary layer

C.P. No. 366
(18,373)
A R.C Technical Report

Printed and published by
HER MAJESTY'S STATIONERY OFFICE

To be purchased from
York House, Kingsway, London W C 2
423 Oxford Street, London W 1
13A Castle Street, Edinburgh 2
109 St Mary Street Cardiff
39 King Street, Manchester 2
Tower Lane, Bristol 1
2 Edmund Street, Birmingham 3
80 Chichester Street, Belfast
or through any bookseller

Printed in Great Britain

S O Code No 23-9010-66

C.P. No. 366